INFECTION AND IMMUNITY, Oct. 2004, p. 5858–5867 Vol. 72, No. 10
0019-9567/04/$08.00+0 DOI: 10.1128/IAI.72.10.5858–5867.2004

Lipoprotein PsaA in Virulence of *Streptococcus pneumoniae*: Surface Accessibility and Role in Protection from Superoxide

Jason W. Johnston,[1] Lisa E. Myers,[2] Martina M. Ochs,[2] William H. Benjamin, Jr.,[3] David E. Briles,[1] and Susan K. Hollingshead[1]*

Department of Microbiology[1] and Department of Pathology,[3] University of Alabama at Birmingham, Birmingham, Alabama, and Department of Microbiology, Aventis Pasteur, Toronto, Ontario, Canada[2]

Received 18 February 2004/Returned for modification 6 April 2004/Accepted 7 July 2004

PsaA of *Streptococcus pneumoniae*, originally believed to be an adhesin, is the lipoprotein component of an Mn^{2+} transporter. Mutations in *psaA* cause deficiencies in growth, virulence, adherence, and the oxidative stress response. Immunofluorescence microscopy shows that PsaA is hidden beneath the cell wall and the polysaccharide capsule and only exposed to antibodies upon cell wall removal. A *psaBC* deletion mutant, expressing PsaA normally, was as deficient in adherence to Detroit 562 cells as were strains lacking PsaA. Thus, PsaA does not appear to act directly as an adhesin, but rather, *psaA* mutations indirectly affect this process through the disruption of Mn^{2+} transport. The deficiency in Mn^{2+} transport also causes hypersensitivity to oxidative stress from H_2O_2 and superoxide. In a chemically defined medium, growth of the wild-type strain was possible in the absence of Fe^{2+} and Mn^{2+} cations after a lag of about 15 h. Addition of Mn^{2+} alone or together with Fe^{2+} allowed prompt and rapid growth. In the absence of Mn^{2+}, the addition of Fe^{2+} alone extended the 15-h lag phase to 25 h. Thus, while Fe^{2+} adversely affects the transition from lag phase to log phase, perhaps through increasing oxidative stress, this effect is relieved by the presence of Mn^{2+}. A scavenger specific for superoxides but not those specific for hydroxyl radicals or H_2O_2 was able to eliminate the inhibition of growth caused by iron supplementation in the absence of Mn^{2+}. This implies that superoxides are a key player in oxidative stress generated in the presence of iron.

The importance of Mn^{2+} for the survival of pathogens during the infectious process has become increasingly apparent in recent years. Mn^{2+} can serve as a cofactor for a variety of bacterial proteins involved in glycolysis, gluconeogenesis, sugar and amino acid metabolism, peptide cleavage, nucleic acid degradation, signal transduction, and oxidative stress defense (27). Mn^{2+} is known to be a cofactor of streptococcal and lactococcal pyruvate kinase and lactate dehydrogenase (13, 24). These enzymes are critical for glycolysis and homolactic fermentation, respectively (13, 24). In *Streptococcus pneumoniae*, Mn^{2+} has been shown to be required for the activity of CpsB, a tyrosine phosphatase involved in the regulation of capsule production (6, 41). In some streptococcal species, lectin-mediated adherence requires Mn^{2+} (16, 37).

Pneumococci possess an ATP-binding cassette (ABC) transporter for Mn^{2+}, the Psa transporter (15, 43). This transporter is composed of the products of three genes, *psaB* (ATP-binding protein), *psaC* (integral membrane protein), and *psaA* (solute-binding lipoprotein), which are organized in an operon with a gene encoding PsaD, a thiol peroxidase (43). PsaA first received attention in pneumococci when it was identified as a potential adhesin and virulence factor (7). *psaA* mutants are known to have a pleiotropic phenotype: reduced adherence to A549 pneumocytes, reduced virulence in multiple infection models, increased sensitivity to oxidative stress, and a requirement for additional Mn^{2+} for growth and competence (7, 15, 38, 60).

PsaA is a member of the lipoprotein receptor-associated antigen I (LraI) family, which includes a number of other streptococcal proteins (12, 29). Included in this group are FimA of *Streptococcus parasanguis*, SsaB of *Streptococcus sanguis*, and ScaA of *Streptococcus gordonii*. While each of these proteins was originally identified as an adhesin, recent work has placed these initial characterizations in doubt. For example, recombinant FimA was suggested to block adherence of *S. parasanguis* to saliva-coated hydroxyapatite, a model for the tooth surface (45), but this finding is compromised by the observation that *fimA* mutants were quite competent in adherence (19). The protein Fap1 of *S. parasanguis* was found to be the relevant adhesin (19, 64). ScaA was believed to be responsible for mediating the coaggregation of *S. gordonii* with *Actinomyces naeslundii* (33); however, *scaA* mutants are not affected in their ability to coaggregate or adhere to fibrin (28). PsaA mutants of *S. pneumoniae* exhibited a reduced ability to adhere to A549 pneumocytes (7); however, purified recombinant PsaA was reported not to block adhesion (43).

The structure of PsaA is not consistent with its putative function as an adhesin. PsaA contains four regions: the leader sequence, two $(\beta/\alpha)_4$ domains, and an α-helical linker (29, 35). The N-terminal leader sequence is 20 amino acids long and contains the LxACy consensus sequence that is recognized by signal peptidase II (29). After cleavage, the cysteine residue is lipid modified, which anchors the protein to the cytoplasmic membrane (29). The remainder of the protein is composed of the two $(\beta/\alpha)_4$ domains linked by the α-helix, forming two lobes with a cleft where the solute-binding site is located (35).

* Corresponding author. Mailing address: Department of Microbiology, BBRB 654/25, University of Alabama at Birmingham, 845 19th St. South, Birmingham, AL 35294. Phone: (205) 934-0570. Fax: (205) 934-0605. E-mail: Hollings@uab.edu.

The overall size of the protein approximated from its crystal structure is 40 by 40 by 70 Å (35). If PsaA is anchored to the cell membrane in its predicted conformation, it should be unable to extend beyond the cell wall and polysaccharide capsule, which is approximately 0.36 μm thick (35, 58). This might be expected to prevent PsaA from functioning directly as an adhesin.

PsaA has been used as an immunogen to elicit protection against pneumococcal disease, the degree of which was observed to vary depending on the type of challenge (7, 12, 36). Initially, intranasal immunization of mice with PsaA was observed to reduce the bacterial load in nasopharyngeal carriage (8, 14). When PsaA was administered in combination with PspA, another immunogenic surface protein, protection against carriage was increased to a greater degree than immunization with PsaA alone (8). Despite the protective effects against carriage, immunization with PsaA consistently failed to protect against systemic infection (44).

Mutations in the *psa* operon result in an almost complete attenuation of virulence for all tested models of animal infection, including respiratory tract, systemic, intraperitoneal chamber, and otitis media models (7, 38). These mutations cause a requirement for added manganese for growth (15). Very low concentrations of Mn^{2+} are available in most in vivo locations (27, 54). Taken together, these results imply that the reduced virulence of *psaA* mutants is most likely due to the reduced availability of Mn^{2+} in the host and that acquisition of Mn^{2+} is essential for survival within the host. Tseng et al. (60) further suggested that virulence attenuation is primarily the result of an inability to regulate oxidative stress and intracellular redox homeostasis on the part of *psaA* mutant strains.

In this paper, we show that PsaA is not exposed on the surface of the bacterial cell, ruling out its function as a direct adhesin. We have extended the studies on the role of Mn^{2+} in protection against oxidative stress and provide evidence that Mn^{2+} assists in protection from internally generated O_2^- and in protection from the Fenton reaction in the presence of Fe^{2+}.

MATERIALS AND METHODS

Bacterial strains, media, and growth conditions. *S. pneumoniae* strain TIGR4 and derivatives thereof were used in this study. Pneumococci were grown at 37°C in Todd-Hewitt broth with 0.5% yeast extract (THY) or on blood agar plates unless otherwise indicated. When appropriate, erythromycin was added to the media at a concentration of 0.3 μg/ml.

During strain construction, plasmids were maintained in *Escherichia coli* TOP10 (Invitrogen, Carlsbad, Calif.) cells grown in Luria-Bertani (LB) broth or on LB plates with 1.5% agar. Ampicillin (50 μg/ml) for pGEM-T- and pCR2.1-based plasmids or erythromycin (400 μg/ml) for pJY4164-based plasmids was added to the growth medium.

For the growth of pneumococci in media with certain metal ion deficiencies, a chemically defined medium (CDM) was prepared as described previously (62), with the exception that divalent cations were withheld. $MgCl_2$ and $CaCl_2$ were added to concentrations of 1 and 0.1 mM, respectively, before use. $MnSO_4$ and $FeSO_4$ were added as specified. Catalase (Worthington Biochem, Lakewood, N.J.), Tiron, and mannitol were added to concentrations of 1,000 U/ml, 5 mM, and 10 mM, respectively, when specified. Growth was monitored by optical density at 600 nm. For growth curves, starter cultures were prepared by growing pneumococci in THY to mid-log phase, washing with CDM, and resuspending cells to an optical density at 600 nm of 0.01 in the desired medium.

Strain construction. The strains, plasmids, and primers used in this study are listed in Table 1. Insertion-duplication (40) was used to inactivate *psaA* and *psaB* in the parental strain TIGR4. Primers JWJ15 and JWJ16 were designed to amplify a 194-bp internal fragment of *psaA*. This fragment was cloned into pCR2.1 with the TOPO TA cloning kit (Invitrogen). Plasmids purified from white colonies were screened by endonuclease digestion with BamHI and XbaI (Promega, Madison, Wis.), and agarose gel electrophoresis was used to determine the presence of the insert. The insert from the resulting plasmid, pJJ028, was subcloned into pJY4164 with BamHI and XbaI sites (66). The resulting plasmid, pJJ034, was transformed into TIGR4.

Primers JWJ75 and JWJ76 were designed to amplify a 299-bp internal fragment of *psaB*. This fragment was cloned into pCR2.1 and subsequently subcloned into pJY4164, creating plasmid pJJ054. This plasmid was used to transform TIGR4 to construct a *psaB* mutant via insertion-duplication mutagenesis (40).

A deletion of *psaBC* was also constructed with a plasmid that contains the region upstream of *psaB* and the region downstream of *psaC*. Primers JWJ65 and JWJ35 were designed to amplify a 1,020-bp region upstream of *psaB*, and primers JWJ79 and JWJ66 were designed to amplify a 390-bp region downstream of *psaC*. These fragments were subcloned into pGEM-T (Promega), creating plasmids pJJ043 and pJJ044, respectively. The insert from pJJ043 was subcloned into pJY4164 with the KpnI and BamHI sites, creating plasmid pJJ045. The insert from pJJ044 was subcloned into pJJ045 with the BamHI and HindIII sites, creating plasmid pJJ046, which was used to transform the *psaB* mutant JEN15 (see below).

Transformation of TIGR4 was performed as described by Yother et al. (67), with modifications. TIGR4 was grown in THY until visible turbidity was present. Bacteria were diluted in competence medium (CTM; THY with 0.2% bovine serum albumin, 0.2% glucose, and 0.02% $CaCl_2$), and 500 ng of competence-stimulating peptide 2 (22) per ml was added to induce competence 14 min prior to the addition of plasmid DNA. The bacteria were incubated at 37°C for 2 h, followed by plating on blood agar containing erythromycin. Resistant transformants were screened for inactivation of the target gene.

PCR with primers JWJ77 and TT1 (*psaA*) or JWJ20 and TT1 (*psaB*) confirmed the integration of the plasmids in the correct locations in the TIGR4 genome. Boiled extracts were prepared from each transformant for use as a template in a PCR. Primers JWJ77 and JWJ20 bind upstream of the plasmid integration site, and TT1 is specific for pJY4164. The *psaB* mutant JEN15 was used to construct a *psaBC* deletion. The *psaA* mutant JEN13 was used for further analysis.

JEN15 was transformed with plasmid pJJ046 to construct a *psaBC* deletion following the protocol outlined above, with minor modifications. Because of the defective transformation ability of *psa* mutants (15), $MnSO_4$ was added to CTM at a concentration of 50 μM. After transformation, bacteria were serially diluted and plated on blood agar without antibiotics. Colonies were screened for the loss of erythromycin resistance to identify transformants. Erythromycin-sensitive colonies were further screened by PCR with primers JWJ20 and JWJ16, which amplify a fragment spanning the *psaBC* region. This primer pair would amplify a 2,279-bp fragment in wild-type TIGR4 and an 804-bp fragment in a deletion strain. The Δ*psaBC* strain JEN16 was used for further analysis.

Anti-PsaA polyclonal antibody production. PsaA was purified as previously described (50) and used to immunize a rabbit to obtain anti-PsaA polyclonal serum. A New Zealand White rabbit (Myrtle's Rabbitry, Thompson Station, Tenn.) was initially injected subcutaneously with 20 μg of PsaA in Freund's complete adjuvant. Five subsequent boosts were performed with Freund's incomplete adjuvant over the following 3 months. The rabbit was bled by cardiac puncture, under anesthesia, 5 months after initial immunization, the blood was allowed to clot, and serum was obtained by centrifugation.

Western blot assay. Equivalent amounts of TIGR4, JEN13, and JEN16 grown in THY to mid-log phase were washed twice with phosphate-buffered saline (PBS), resuspended in PBS with sodium dodecyl sulfate (SDS)-polyacrylamide gel electrophoresis (PAGE) sample buffer, and boiled for 5 min. Samples and a low-range biotinylated SDS-PAGE standard (Bio-Rad, Hercules, Calif.) were loaded onto a NuPAGE 10% Bis-Tris gel (Invitrogen) and separated by electrophoresis in morpholineethanesulfonic acid (MES)-SDS running buffer (Invitrogen) in accordance with the manufacturer's instructions. Proteins were then transferred to a nitrocellulose membrane with the Trans-Blot SD semidry transfer cell (Bio-Rad). The blot was probed with anti-PsaA polyclonal antibody diluted 1:1,000 in PBS with 1% bovine serum albumin. Goat anti-rabbit immunoglobulin G (heavy and light chains)-alkaline phosphatase and streptavidin-alkaline phosphatase (Southern Biotechnology Associates, Inc., Birmingham, Ala.) were used as the secondary antibody and for detection of the marker, respectively. Colorimetric detection was performed with Sigma Fast nitroblue tetrazolium–5-bromo-4-chloro-3-indolylphosphate (NBT-BCIP) tablets (Sigma-Aldrich, St. Louis, Mo.).

Production of protoplasts. Protoplasts were produced with the method described by Yother and White (68). Cells were pelleted and washed once with H_2O. The pellet was then resuspended in protoplast buffer (20% sucrose, 5 mM Tris [pH 7.4], 2.5 mM $MgSO_4$), and 10 U of mutanolysin (Sigma-Aldrich) was

TABLE 1. Strains, plasmids, and primers used in this study

Strain, plasmid, or primer	Relevant characteristics or sequence and gene	Source or reference
Strains		
S. pneumoniae		
TIGR4	Wild-type, capsule type 4, transparent variant	57
JEN13	TIGR4 *psaA*::Erm, transparent variant	This study
JEN15	TIGR4 *psaB*::Erm	This study
JEN16	JEN15 Δ*psaBC*, transparent variant	This study
TIGR1001.1	*cps*::Erm, capsule negative	This study
E. coli TOP10	General cloning strain	Invitrogen
Plasmids		
pCR2.1	3.9 kb, Amp^r, ColE1 *ori*	Invitrogen
pGEM-T	3.0 kb, Amp^r, ColE1 *ori*	Promega
pJY4164	4.4 kb, Erm^r, ColE1 *ori*	66
pJJ028	pCR2.1 with an internal *psaA* fragment; Amp^r	This study
pJJ034	pJY4164 with an internal *psaA* fragment; Erm^r	This study
pJJ043	pGEM-T with fragment upstream of *psaB;* Amp^r	This study
pJJ044	pGEM-T with fragment downstream of *psaC;* Amp^r	This study
pJJ045	pJY4164 with fragment upstream of *psaB;* Erm^r	This study
pJJ046	pJJ045 with fragment downstream of *psaC;* Erm^r	This study
pJJ052	pCR2.1 with an internal *psaB* fragment; Amp^r	This study
pJJ054	pJY4164 1,410-bp fragment fusing partial *psaB* and psaC genes; Erm^r	This study
Primers[a]		
JWJ15	GCAAGACCCACACGAATACGAAC; *psaA*	This study
JWJ16	CAAGGTAGATAACATCAACGCCG; *psaA*	This study
JWJ20	CGTGTCATCTTGTTCTCGC; *psaB* upstream	This study
JWJ35	ggatccGGAGACACTGAGGTTTTCG; *psaB* upstream	This study
JWJ65	ggtaccTGAAGAAGTCATCCAAAGGTAGGG; *psaB* upstream	This study
JWJ66	aagcttGTAAACCAAGCATTGCCACC; *psaC* downstream	This study
JWJ75	TTATCCCACATCAAGGTCAGGC; *psaB*	This study
JWJ76	CACCAAACATCTGGCAATCAAGAC; *psaB*	This study
JWJ77	CCTTTTCTTCTTTCTTAGCCCTCG; *psaC*	This study
JWJ79	ggatccTTTATCGCTCCCAAACAAC; *psaC* downstream	This study
TT1	GCCACTATCGACTACGCG	

[a] Primers were based on the complete genome sequence of *S. pneumoniae* TIGR4 (57). Lowercase denotes mismatches used to create restriction endonuclease sites. All sequences are expressed 5′ to 3′.

added. The suspension was incubated overnight at room temperature. The formation of protoplasts was confirmed by microscopic examination. Protoplasts were pelleted, resuspended in protoplast buffer, and used for immunofluorescence microscopy.

Immunofluorescence microscopy. Log-phase cells were pelleted, washed twice with PBS, resuspended in PBS with 1% bovine serum albumin (PBSB), and incubated at room temperature for 20 min. Cells were pelleted and resuspended in PBSB or anti-PsaA serum diluted 1:100 in PBSB and incubated at 37°C for 30 min followed by two washes with PBS. Cells were then incubated with goat anti-rabbit immunoglobulin G (heavy and light chains)-fluorescein isothiocyanate (Southern Biotechnology Associates, Inc.) diluted in PBSB at 4°C for 30 min. Cells were washed twice with PBS and resuspended in 4% formaldehyde. Protoplasts were prepared similarly except that all buffers contained 20% sucrose. Bacterial cells were viewed by fluorescence microscopy as described previously (46).

Tissue culture. Detroit 562 (D562) human pharyngeal carcinoma cells (CCL-138; American Type Culture Collection, Manassas, Va.) were maintained and passages were grown in minimal essential medium (MEM) without L-glutamine, supplemented with Earle's salts and 2.2 g of sodium bicarbonate (Gibco, Grand Island, N.Y.) per liter, 0.1 mM nonessential amino acids (Gibco), 1.0 mM sodium pyruvate (Gibco), 2.0 mM L-glutamine (Gibco), and 10% heat-inactivated fetal bovine serum (JRH Biosciences, Lenexa, Kans.) (supplemented MEM). Flat-bottom 96-well tissue culture-treated plates (Becton Dickinson Labware, Franklin Lakes, N.J.) were seeded with approximately 2×10^4 D562 cells/well and cultured at 37°C under 5% CO_2 to form confluent monolayers. Monolayers used for the assays were typically 4 to 6 days old.

Adherence assay. Before use, monolayers were washed once with 200 μl of supplemented MEM per well. The medium was aspirated off, and 50 μl of supplemented MEM was added to each well. Frozen stocks of *S. pneumoniae* TIGR4 and derivatives thereof were removed from −70°C and thawed at room temperature. Serial $\log_{10}$ dilutions of bacterial stocks were prepared in supplemented MEM to a final volume of 2.0 ml in 6.0-ml polypropylene tubes. To obtain an estimate of CFU added per well, each strain was further diluted 10-fold in Dulbecco's PBS (Gibco) supplemented with 0.2% bovine serum albumin (Sigma-Aldrich) to a final volume of 100 μl in 96-well round-bottom non-tissue culture-treated plates (Becton Dickinson Labware). Each sample dilution was prepared in duplicate. A 40-μl volume of each diluted sample was plated onto Trypticase soy agar (TSA II) plates containing 5% sheep blood (Becton Dickinson Biosciences, Cockeysville, Md.) and incubated overnight at 37°C under 5% CO_2. Each bacterial strain was tested at four to five dilution points within a range of 10^3 to 2×10^8 CFU added/well.

For adherence assay plates, 50 μl of appropriately diluted bacteria in supplemented MEM was added to triplicate wells of a 96-well plate containing washed D562 monolayers. After a 2.5-h incubation at 37°C under 5% CO_2, monolayers were washed five times with 200 μl of PBS supplemented with 0.2% bovine serum albumin/well to remove nonadherent bacteria. D562 cells were detached by the addition of 20 μl of 0.05% trypsin with 0.53 mM EDTA-Na_4 (Gibco) /well. After 10 min at 37°C, each sample well was neutralized with 80 μl of supplemented MEM, and samples were mixed by pipetting up and down 50 times with a Biohit Proline electronic pipettor (Biohit, Helsinki, Finland) set to a 55-μl volume and maximum speed mixing mode. Tenfold plating dilutions of each sample were prepared in PBS with 0.2% bovine serum albumin to a final volume

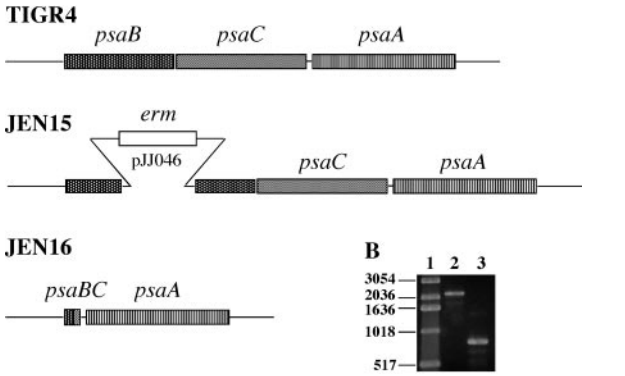

FIG. 1. Construction of *psa* mutants. (A) The wild-type strain TIGR4 contains an intact *psa* operon. JEN15 (*psaB*) has an insertion-duplication mutation in *psaB*, created with plasmid pJJ046. JEN16 has the majority of *psaB* and *psaC* deleted, with a 30-residue fusion protein. (B) PCR products amplified with primers that span the *psa* operon. Lane 1, 1-kb DNA ladder (Invitrogen); lane 2, TIGR4; lane 3, JEN16.

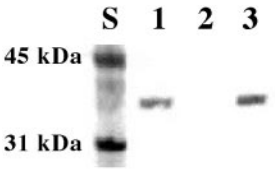

FIG. 2. Western blot assay for PsaA expression. Whole-cell lysates were separated by SDS-PAGE, transferred to nitrocellulose blots, and probed with anti-PsaA antiserum. PsaA runs at 37 kDa. Lane 1, TIGR4; lane 2, JEN13 (*psaA*); lane 3, JEN16 (Δ*psaBC*). The procedure used is described in Materials and Methods.

of 100 μl in 96-well round-bottom non-tissue culture-treated plates (Becton Dickinson Labware). A volume of 40 μl of each diluted sample was plated onto TSA II agar plates containing 5% sheep blood. Agar plates were incubated for 18 to 36 h at 37°C under 5% CO_2. The CFU per plate were counted under magnification. The average CFU count of replicate plates was used to estimate the number of CFU added per well and the number of CFU bound per well.

Intravenous infection of mice. Six- to 12-week-old female CBA/CaHN-*Btk*^{xid}/J (CBA/N) mice were obtained from Jackson Laboratories (Bar Harbor, Maine). The virulence of pneumococci was examined with a systemic model of infection as described previously (52). Mice were injected with 300 to 1,000 CFU diluted in Ringer's solution, and survival time was monitored.

Oxidative stress sensitivity. To determine the sensitivity of pneumococcal strains to H_2O_2, log-phase pneumococcal cultures grown in THY broth were treated with 0, 0.1, 1, 10, and 40 mM H_2O_2 and incubated at 37°C for 30 min. Percent survival was determined by obtaining CFU counts from dilution plating. The assay was performed in triplicate.

To determine the sensitivity of pneumococcal strains to superoxide, log-phase cultures grown in THY broth were treated with 50 mM paraquat, a generator of intracellular superoxide, to obtain a survival curve. Untreated cultures were used as a negative control. At defined time points, samples were removed from treated and untreated cultures and plated to obtain CFU counts. The assay was performed in triplicate.

RESULTS

Construction of *psaA and* Δ*psaBC* strains. Insertion-duplication mutagenesis (40) was used to create *psaA* and *psaB* mutants of strain TIGR4 (Fig. 1A). The *psaB* mutant JEN15 was used to create JEN16, a Δ*psaBC* strain that still expressed *psaA* (Fig. 1A). A plasmid was constructed with a 1.4-kb insert containing a 1,020-bp fragment including 30 bp at the 5′ end of *psaB* fused to a 390-bp fragment including the last 54 bp of *psaC*, which, when ligated together, would encode an in-frame, 30-amino-acid fusion protein, PsaBC. This plasmid, pJJ054, was transformed into JEN15, and double-crossover events were screened for by the loss of erythromycin resistance. The deletion was confirmed by PCR with primers that span the *psa* operon (Fig. 1B). This primer pair amplifies a 2,279-bp fragment from the wild-type strain and an 804-bp product from the deletion strain, JEN16.

Western blot analysis was used to confirm that JEN16 expressed PsaA in an amount comparable to that of the TIGR4 parent strain (Fig. 2). The anti-PsaA polyclonal antiserum used to develop the Western blot bound a 37-kDa protein in TIGR4 and JEN16 lysates, while this band was absent in the *psaA* mutant JEN13 (Fig. 2). The Δ*psaBC* strain JEN16 was used for further investigation of the role of the PsaA protein itself compared to its role as part of an active transporter for Mn^{2+}.

PsaA is not exposed on the cell surface of intact *S. pneumoniae*. The anti-PsaA serum was also used to determine if PsaA was exposed on the surface of pneumococci. Because of reported surface differences between transparent and opaque phase variants of pneumococci (32), we examined TIGR4 strains that were 99% transparent. Log-phase cells from transparent variants of TIGR4, *psaA*, and Δ*psaBC* strains were compared to protoplasts produced from the same cultures. Samples were stained with anti-PsaA followed by fluorescein isothiocyanate-conjugated anti-rabbit immunoglobulin and then examined by immunofluorescence microscopy. Antibodies did not label intact cells. No detectable fluorescence was observed in any of the strains tested (Fig. 3). What little fluorescence was present in whole-cell samples was not found associated with any of the cells detected by light microscopy but rather was associated with what appeared to be cellular debris (Fig. 3). Additionally, PsaA was not exposed in TIGR1001.1, a strain defective in capsule production, indicating that PsaA is completely covered by the cell wall (results not shown). Detection of PsaA with the anti-PsaA serum was only observed when the cell wall was removed from the TIGR4 and from the Δ*psaBC* strain to make protoplasts (Fig. 3). The protoplasts of the *psaA* mutant strain exhibited no fluorescence (data not shown). These results indicate that PsaA is normally not accessible to anti-PsaA antibodies on the cell surface, an observation which suggests that PsaA may also not be sufficiently exposed to function as a structural adhesin.

Δ*psaBC* mutant is defective in adherence. If PsaA is indeed not exposed on the cell surface, then it is possible that the requirement of PsaA for colonization and virulence is the result of the loss of the high-affinity Mn^{2+} transport system. To test this possibility, we compared the effects of the *psaA* mutation and the Δ*psaBC* deletion on adherence. Neither of these bacteria should have a functioning Psa Mn^{2+} transport pathway, but the Δ*psaBC* mutant, like TIGR4, expresses PsaA. Previously, adherence of *psaA* mutants to A549 cells, a lung pneumocyte cell line, had been found to be reduced to 10% of wild-type levels (7). Binding curves were obtained for TIGR4, *psaA*, and Δ*psaBC* strains (Fig. 4). There was a similar 10-fold reduction in the adherence of both the Δ*psaBC* (even though PsaA is expressed) and the *psaA* mutant strains compared to

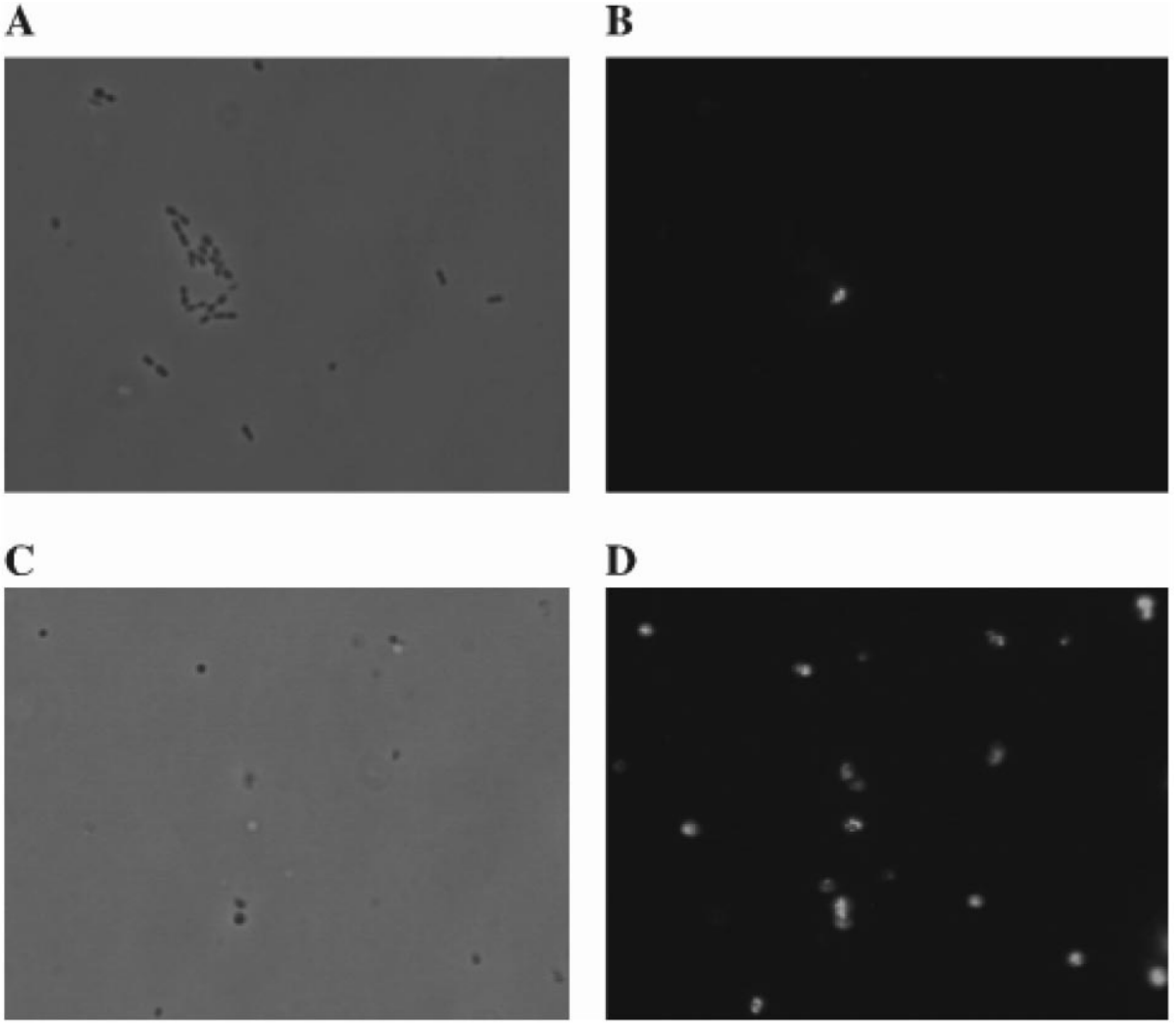

FIG. 3. Immunofluorescence microscopy. Intact TIGR4 cells were viewed by phase-contrast (A) and confocal (B) microscopy. Protoplasts made from TIGR4 were viewed by phase-contrast (C) and confocal (D) microscopy. Samples were stained with rabbit anti-PsaA followed by anti-rabbit immunoglobulin conjugated to fluorescein isothiocyanate.

that of TIGR4 (Fig. 4). The binding curve for the Δ*psaBC* mutant was nearly identical to that for the *psaA* mutant.

The decreased adherence of both mutants indicates that it is not the absence of PsaA that decreases the adherence of PsaA$^-$ mutants but suggests that it is the absence of the Psa Mn^{2+} transport pathway. These results argue that expression of PsaA is not sufficient for adherence. Taken together, the inaccessibility of PsaA and the reduced adherence of the Δ*psaBC* strain implicate the transport of Mn^{2+} as the cause of the pleiotropic phenotype seen in *psa* mutants.

Δ*psaBC* mutant is attenuated in virulence. To determine if the Δ*psaBC* mutant exhibits attenuated virulence, the TIGR4 and Δ*psaBC* strains were tested in a model of systemic pneumococcal infection. Approximately 300 CFU were injected intravenously into CBA/N mice, and survival of the mice was monitored. A majority of mice infected with TIGR4 became moribund by 4 days postinfection, and all had become moribund by day 7. Mice infected with the Δ*psaBC* mutant survived

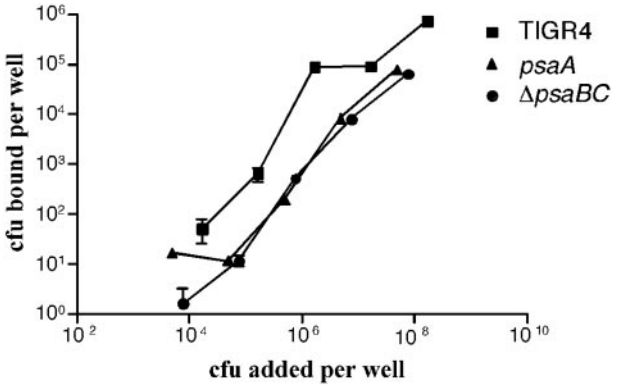

FIG. 4. Adherence of TIGR4 (squares), *psaA* (triangles), and Δ*psaBC* (circles) strains to D562 nasopharyngeal cells. The assay was performed with confluent D562 monolayers. Serial dilutions of TIGR4, Δ*psaBC*, and *psaA* strains were added to triplicate wells and incubated for 2.5 h at 37°C under 5% CO_2. The wells were washed, and the cells were detached prior to dilution plating to determine the CFU bound per well.

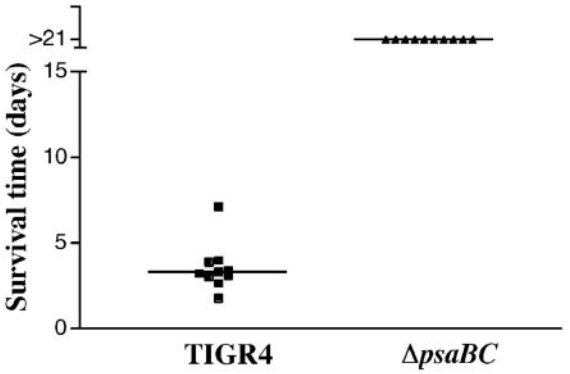

FIG. 5. Virulence of TIGR4 and Δ*psaBC* strains in a mouse model for systemic infection. Mice were infected intravenously, and survival time was monitored. The horizontal line designates the median time until the mice became moribund.

the infection (Fig. 5), indicating complete attenuation of virulence in this strain.

Δ*psaBC* mutant is hypersensitive to oxidative stress. Previous work determined that *psaA* mutants exhibit increased sensitivity to oxidative stress (60). The relative abilities of the Δ*psaBC* strain to survive H_2O_2- and superoxide (O_2^-)-induced oxidative stress were examined. Decreased survival of the Δ*psaBC* mutant was observed at H_2O_2 concentrations ranging from 0.1 to 40 mM compared to the wild type (Fig. 6A). With 50 mM paraquat as a generator of O_2^-, survival curves of the two strains were generated (Fig. 6B). While the wild-type strain was sensitive to paraquat, the Δ*psaBC* strain exhibited increased sensitivity. After 90 min of treatment with paraquat, all of the Δ*psaBC* strain pneumococci were killed, whereas 0.01% of the wild type survived (Fig. 6B). Taken together, these data indicate that the Δ*psaBC* mutant is highly susceptible to oxidative stress, as had been previously reported for the *psaA* mutant. Thus, it is clear that it is the loss of the transport pathway (15), and not just the loss of PsaA, that causes the sensitivity to oxidative stress. We note that is unlikely that the expression of PsaD is adversely affected in our Δ*psaBC* mutant.

Requirement of Mn^{2+} for pneumococcal growth. To further investigate the role of Mn^{2+} transport in pneumococci, the requirement of Mn^{2+} for growth was examined. Previously, mutations in all three genes of the *psa* transporter have resulted in attenuated growth, even in the presence of additional Mn^{2+} (15, 38). To confirm the growth defect in the Δ*psaBC* strain, TIGR4 and the Δ*psaBC* strain were grown in THY (Fig. 7A). As expected, the growth of Δ*psaBC* was attenuated compared to that of the wild type. This indicates that the normal function of the *psa* transporter is required for wild-type growth of pneumococci in this medium.

Since prior studies have implicated this transporter for the transport of Mn^{2+}, we examined the effect of Mn^{2+} on the growth of the mutant. Growth was examined in a chemically defined medium (CDM) that contains all the nutrients needed for robust growth and allows strict control of metal ion concentrations. In CDM (containing Mg^{2+} and Ca^{2+}) with Mn^{2+} (0.1 or 50 μM), TIGR4 and the Δ*psaBC* mutant had comparable growth at 50 μM Mn^{2+}, while growth of the mutant was attenuated at 0.1 μM Mn^{2+}, indicating that the high concentration of Mn^{2+} was required for optimal growth (Fig. 7B). These data suggest the presence of a second transporter for Mn^{2+} that is functional at high extracellular concentrations of Mn^{2+}.

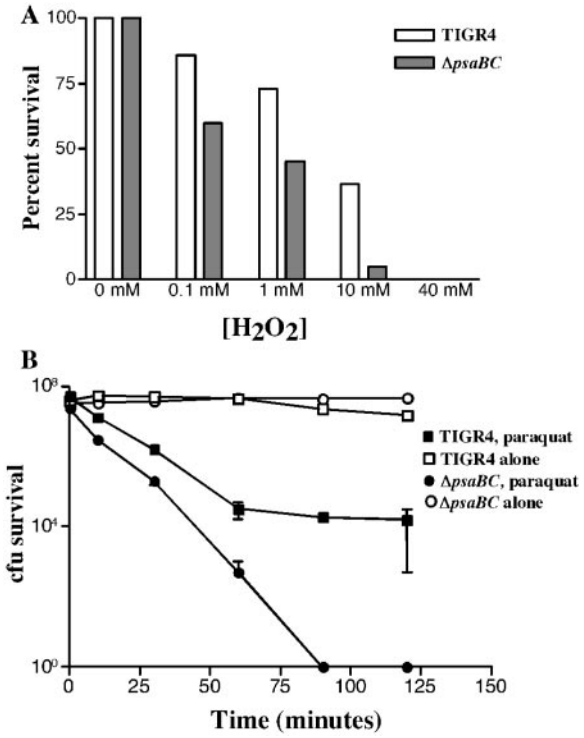

FIG. 6. Oxidative stress response. (A) TIGR4 (open bars) and Δ*psaBC* (solid bars) were treated with various concentrations of H_2O_2 for 30 min, and percent survival was determined. (B) TIGR4 (squares) and Δ*psaBC* (circles) were incubated with 50 mM paraquat (solid symbols) or without (open symbols), and the number of surviving CFU was determined at various time points. Both assays were performed in triplicate.

If the impairment of Mn^{2+} transport in the Δ*psaBC* strain affects growth, then the growth of the wild-type strain should be similarly affected in Mn^{2+}-depleted conditions. This was examined with CDM (containing Mg^{2+} and Ca^{2+}) with Mn^{2+} (0.1 or 50 μM) and/or Fe^{2+} (50 μM) (Fig. 8). Without the addition of either Mn^{2+} or Fe^{2+}, TIGR4 grew after an extended lag phase (≈15 h), and a doubling time (T_D) of 48.6 min was observed in log phase. When 50 μM Fe^{2+} was added to the medium in the absence of Mn^{2+}, the lag phase was increased to 24 h before log phase growth (T_D of 29.5 min). The addition of Mn^{2+} alone reduced the lag phase to 5 h, and growth in both concentrations of Mn^{2+} was comparable. The addition of both 0.1 μM Mn^{2+} and 50 μM Fe^{2+} reduced the lag phase to 18 h compared to that with Fe^{2+} alone, while the addition of 50 μM Mn^{2+} completely counteracted the effects of Fe^{2+}, reducing the lag phase to 5 h. These results indicate that Fe^{2+} may be toxic to pneumococci in the absence of Mn^{2+} and that the presence of Mn^{2+} allows a reduced duration of lag-phase growth.

In the presence of oxygen, Fe^{2+} is known to react with H_2O_2 to produce the highly toxic hydroxyl radical species ($OH^{\cdot}$) in the Fenton reaction (49). Thus, the toxicity of Fe^{2+} may be due

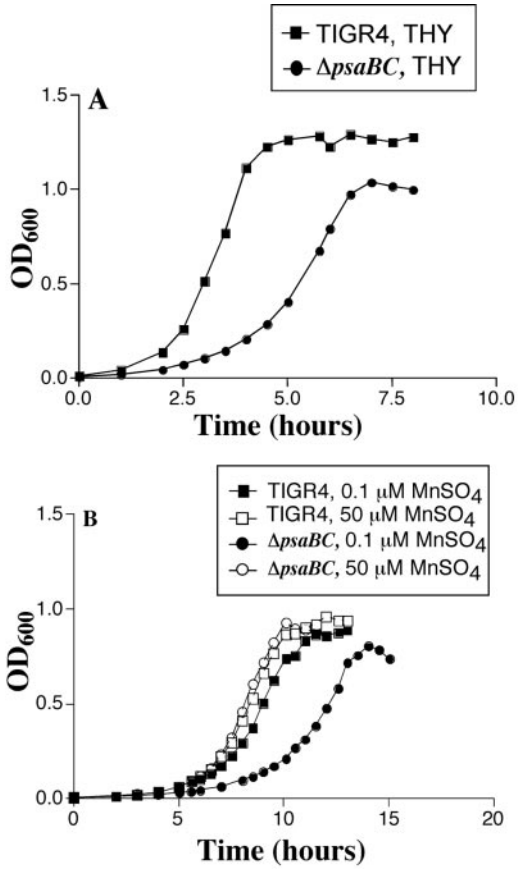

FIG. 7. Growth of TIGR4 (squares) and Δ*psaBC* (circles) strains: (A) growth curves of TIGR4 and Δ*psaBC* in THY; (B) growth curves of TIGR4 and Δ*psaBC* grown in CDM with 0.1 μM $MnSO_4$ (solid symbols) or 50 μM $MnSO_4$ (open symbols). Results are representative of multiple experiments.

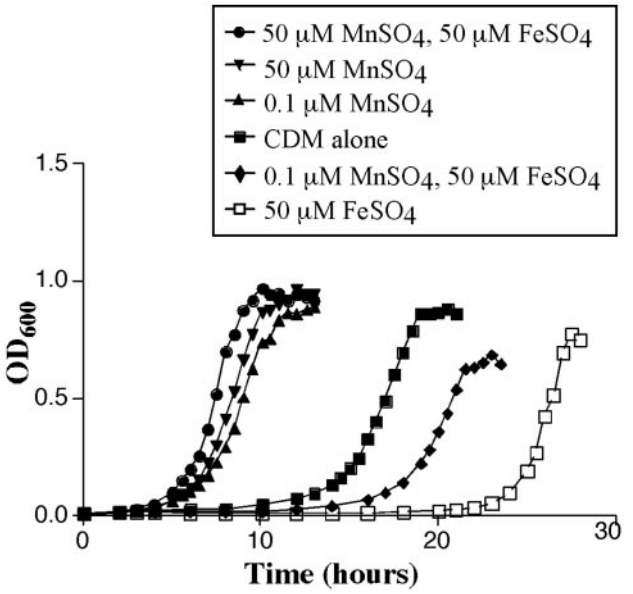

FIG. 8. Growth of TIGR4 in CDM. TIGR4 was grown in CDM alone (squares) or supplemented with 0.1 μM $MnSO_4$ (upward triangles), 50 μM $MnSO_4$ (downward triangles), 0.1 μM $MnSO_4$ and 50 μM $FeSO_4$ (diamonds), 50 μM $MnSO_4$ and 50 μM $FeSO_4$ (circles), or 50 μM $FeSO_4$ (open squares). Results are representative of multiple experiments.

to its participation in this reaction in aerobic conditions. Mn^{2+} is known to detoxify reactive oxygen species and is also the cofactor of superoxide dismutase (SodA) of pneumococci (11, 65). To determine if the presence of reactive oxygen species contributes to the impaired growth of pneumococci in the absence of Mn^{2+}, growth was examined with scavengers for H_2O_2 (catalase) or for superoxide (tiron) or for hydroxyl radicals (mannitol) (1). When TIGR4 was grown in the presence of Tiron, in the absence of Mn^{2+}, the lag phase was reduced to 5 h, even in the presence of iron (Fig. 9). Catalase (1,000 U/ml) and mannitol (10 mM) did not significantly affect the length of the lag phase (data not shown), suggesting that superoxide toxicity is primarily responsible for the increased delay in growth in the absence of Mn^{2+}. Growth in the presence of Tiron (5 mM) but without Mn^{2+} was comparable to growth in the presence of Mn^{2+} but without Tiron, implying that the main role of Mn^{2+} in growth is the detoxification of superoxide. Additional experiments with methylene blue as an indicator of anaerobic conditions yielded the observation that pneumococcal cultures enter log-phase growth after the O_2 is cleared from the medium and the conditions are essentially anaerobic (data not shown).

DISCUSSION

It has long been accepted that the acquisition of iron can be crucial for some pathogens in the iron-limited environment of the host. However, many of the key enzymes that require iron are involved in cellular respiration or participate in the tricarboxylic acid cycle. Many gram-positive bacteria in the lactic acid bacterial group are incapable of respiration and use fermentation exclusively to generate energy. Pathogens that have eliminated or at least reduced the need for iron would have a selective advantage in the host, where iron is not readily available. Some pathogens are known to dispense with iron dependency and rely on Mn^{2+} for the metal ion needs of the cell (2, 36, 42, 51, 63). Mn^{2+} has multiple roles in the survival and growth of pathogens (27). Mn^{2+} demands a high-affinity transporter for its acquisition in limiting environments within the host. Pneumococci possess the Psa transport system, a putative Mn^{2+} ABC transporter that is required for virulence (7, 43). Inactivation of the *psa* operon leads to a pleiotropic phenotype, including defects in growth, competence, adherence, virulence, and defense against oxidative stress (15, 38, 60).

In the current study, PsaA was found to be inaccessible to antibody on the cell surface unless the cell wall was digested with mutanolysin to produce protoplasts. The cell wall for gram-positive bacteria has been estimated to span 40 nm (20) and to be impermeable to molecules >10 kDa in size (39, 55). The inability to bind whole cells with anti-PsaA antibodies is in contradiction to the results presented by Russell et al., who saw labeling of cells with an anti-PsaA monoclonal antibody (53). However, the harsh treatments of pneumococci in their study, including acetone washes and potentially partial autolysis, may have damaged the integrity of the capsule and cell wall before

the application of the antibody. In the present study, encapsulated pneumococci, unencapsulated pneumococci, and protoplasts were incubated with anti-PsaA antibodies. Labeling of whole cells was only observed when the cell wall was removed, indicating that PsaA is buried beneath both the polysaccharide capsule and the cell wall. This result is consistent with the known globular structure of PsaA (35) and its lipid-based anchoring to the membrane. The adherence of a strain with *psaBC* deleted but still expressing PsaA was found to be attenuated, similar to that of *psaA* mutants. Deletion of *psaBC* also resulted in complete attenuation of virulence in a systemic model of infection. These results make it unlikely that PsaA functions directly as an adhesin but instead point to the limitation of intracellular Mn^{2+} as being responsible for the phenotypes observed in *psa* mutants.

The defect in growth caused by impaired Mn^{2+} transport may be due to the reduced capacity to defend against oxidative stress generated by metabolism (60). Pneumococci produce a significant amount of H_2O_2 during growth, mainly due to the presence of pyruvate oxidase (56). This production of H_2O_2 is believed to be important in the virulence of pneumococci and as a mechanism to eliminate competition by other pathogens (17, 47). In the Fenton reaction, H_2O_2 reacts with Fe^{2+} to produce the hydroxyl radical, which can cause a variety of cellular damages (49). Superoxide, O_2^-, can then react with Fe^{3+} to regenerate Fe^{2+}, which is then ready to react with another H_2O_2 molecule (59). Mechanisms to detoxify these molecules, which are produced as a consequence of metabolism (60), are necessary. Pneumococci do not produce catalase but do make an Mn^{2+}-dependent superoxide dismutase (SodA) and a thiol peroxidase (PsaD), both of which are required for full virulence (7, 65).

It appears that Mn^{2+} is required to deal with the oxidative stress created by the metabolism of pneumococci and exacerbated by Fe^{2+}. Growth of pneumococci in the presence of Fe^{2+} alone resulted in a dramatically increased lag phase, presumably due to the Fenton reaction, while the addition of Mn^{2+} alleviated this effect, reducing the lag phase significantly. Mn^{2+} can function as an antioxidant, detoxifying both H_2O_2 and superoxide (3, 4, 25). Pneumococci possess an enzyme that is responsible for the reduction of O_2, NADH oxidase (Nox) (5). This enzyme is believed to function to reduce molecular oxygen to prevent the formation of reactive oxygen species (69). Mutants defective in Nox are unable to grow under vigorous aeration; however, they are able to grow in static cultures (23, 69). The presence of O_2 and the resulting reactive oxygen species inhibit log-phase growth in pneumococci. Our results indicate that clearance of O_2 and reactive oxygen species from the medium are required for the transition of pneumococci from lag-phase to log-phase growth and that Mn^{2+} allows this process to proceed efficiently, while Fe^{2+} hinders it.

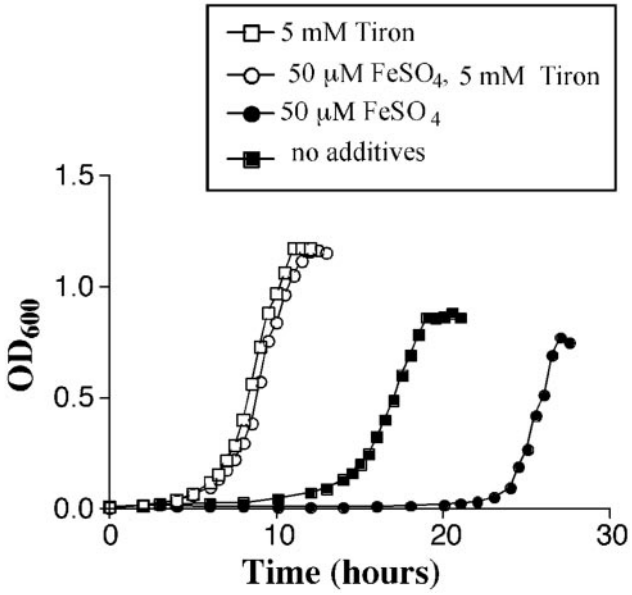

FIG. 9. Effect of Tiron on growth. TIGR4 was grown in CDM alone with no $MnSO_4$ (solid squares), or with 50 μM $FeSO_4$ (solid circles). Tiron (5 mM) was added to the CDM with no $MnSO_4$ (open squares) and the same medium with 50 μM $FeSO_4$ (open circles). The results are representative of at least three independent experiments.

Superoxide appears to be the major inhibitor of the transition from lag- to log-phase growth in pneumococci. Growth of wild-type pneumococci was improved by the addition of tiron, a superoxide scavenger, to the growth medium. Neither catalase, which removes H_2O_2, nor mannitol, which can detoxify hydroxyl radicals, was able to augment growth. In this system, superoxide was primarily responsible for the increased lag phase. The presence of Mn^{2+} also decreased the duration of the lag phase, demonstrating a role for Mn^{2+} in detoxifying superoxide. The mechanism by which superoxide inhibits growth is incompletely understood. Superoxide is less reactive than H_2O_2 or the hydroxyl radical and is unable to attack DNA directly (59). It is, however, able to potentiate the production of hydroxyl radicals via releasing free intracellular Fe^{2+} which can participate in the Fenton reaction (59). Superoxide releases Fe^{2+} by freeing it from enzymes containing labile $[4Fe\text{-}4S]^{2+}$ clusters, simultaneously inactivating the enzymes and causing metabolic defects in the associated pathways and growth defects in *Escherichia coli* (18, 26, 30, 31, 34). While pneumococci appear to lack many of the enzymes carrying $[4Fe\text{-}4S]^{2+}$ from which Fe^{2+} can be leached (48, 57), they do have the enzymes dihydroxy-acid dehydratase and transketolase, which have been shown to be susceptible to damage by superoxides in other organisms (26).

It was curious that mannitol did not significantly affect growth in the absence of Mn^{2+}. If superoxide increases the production of hydroxyl radicals, then it would be expected that protection against hydroxyl radicals would also improve growth. Similarly, scavenging of H_2O_2 did not augment growth. This may imply a more direct role for superoxide in cellular toxicity. The need to repair enzymes whose labile $[4Fe\text{-}4S]^{2+}$ clusters had been damaged by superoxide could contribute to the lag before growth begins. Then, the role for Mn^{2+} might be to scavenge superoxide before this damage can occur. This is consistent with recent findings on the role of Mn^{2+} and superoxide detoxification aside from the cofactoring of Sod enzymes (21, 61). Recent work by Pericone et al. demonstrated relative resistance of *S. pneumoniae* to the killing effects of the Fenton reaction (48). It is possible that part of this resistance derives from internal stores of Mn^{2+} brought into the cell by the Psa transporter.

If iron is toxic to pneumococci, why is it taken up at all? Up

to three iron ABC transporters are present in the pneumococcal genome (9, 10). This indicates that iron does play an important role in the metabolism and virulence of pneumococci, otherwise evolution would have likely eliminated multiple iron transporters. It is important to note that while the inactivation of the Psa transporter completely attenuates virulence, the inactivation of two of the three iron ABC transporters only moderately attenuated virulence (10). The relative importance of Mn^{2+} and Fe^{2+} to the virulence of pneumococci cannot be directly compared yet because studies have not looked at the virulence of a triple mutant that is deficient in all three iron transporters.

Mn^{2+} likely has multiple functions in pneumococci. *sodA* mutants are only partially attenuated in virulence in pneumonia models of infection and unaffected in systemic models of infection (65). In contrast, *psa* mutants, which lack Mn^{2+} transport, are completely attenuated in all models of infection (7, 38). This may be a result of the reduced growth rate of pneumococci due to Mn^{2+} limitation in vivo. It is possible that Mn^{2+} may function in a detoxifying mechanism that is independent of its role as a cofactor in SodA. Regardless, the importance of an active, high-affinity transporter for Mn^{2+} in the virulence of pneumococci is clear.

ACKNOWLEDGMENTS

We thank James Paton for the generous gift of recombinant PsaA, John Kearney for assistance with the immunofluorescence microscopy, and Hazeline Roche for construction of the capsule-negative TIGR4 strain.

These studies were conducted with support from NIH grants AI21458 and AI40645. Jason Johnston was supported by NIAID training grant T32 AI 07041.

REFERENCES

1. **Andre, P., S. Bilger, P. Remy, S. Bettinger, and D. J. Vidon.** 2003. Effects of iron and oxygen species scavengers on *Listeria* spp. chemiluminescence. Biochem. Biophys. Res. Commun. **304:**807–811.
2. **Aranha, H., R. C. Strachan, J. E. Arceneaux, and B. R. Byers.** 1982. Effect of trace metals on growth of *Streptococcus mutans* in a Teflon chemostat. Infect. Immun. **35:**456–460.
3. **Archibald, F. S., and I. Fridovich.** 1981. Manganese and defenses against oxygen toxicity in *Lactobacillus plantarum*. J. Bacteriol. **145:**442–451.
4. **Archibald, F. S., and I. Fridovich.** 1982. The scavenging of superoxide radical by manganous complexes: in vitro. Arch. Biochem. Biophys. **214:**452–463.
5. **Auzat, I., S. Chapuy-Regaud, G. Le Bras, D. Dos Santos, A. D. Ogunniyi, I. Le Thomas, J. R. Garel, J. C. Paton, and M. C. Trombe.** 1999. The NADH oxidase of *Streptococcus pneumoniae*: its involvement in competence and virulence. Mol. Microbiol. **34:**1018–1028.
6. **Bender, M. H., and J. Yother.** 2001. CpsB is a modulator of capsule-associated tyrosine kinase activity in *Streptococcus pneumoniae*. J. Biol. Chem. **276:**47966–47974.
7. **Berry, A. M., and J. C. Paton.** 1996. Sequence heterogeneity of PsaA, a 37-kilodalton putative adhesin essential for virulence of *Streptococcus pneumoniae*. Infect. Immun. **64:**5255–5262.
8. **Briles, D. E., E. Ades, J. C. Paton, J. S. Sampson, G. M. Carlone, R. C. Huebner, A. Virolainen, E. Swiatlo, and S. K. Hollingshead.** 2000. Intranasal immunization of mice with a mixture of the pneumococcal proteins PsaA and PspA is highly protective against nasopharyngeal carriage of *Streptococcus pneumoniae*. Infect. Immun. **68:**796–800.
9. **Brown, J. S., S. M. Gilliland, and D. W. Holden.** 2001. A *Streptococcus pneumoniae* pathogenicity island encoding an ABC transporter involved in iron uptake and virulence. Mol. Microbiol. **40:**572–585.
10. **Brown, J. S., S. M. Gilliland, J. Ruiz-Albert, and D. W. Holden.** 2002. Characterization of *pit*, a *Streptococcus pneumoniae* iron uptake ABC transporter. Infect. Immun. **70:**4389–4398.
11. **Cheton, P. L., and F. S. Archibald.** 1988. Manganese complexes and the generation and scavenging of hydroxyl free radicals. Free Radic. Biol. Med. **5:**325–333.
12. **Claverys, J. P.** 2001. A new family of high-affinity ABC manganese and zinc permeases. Res. Microbiol. **152:**231–243.
13. **Crow, V. L., and G. G. Pritchard.** 1977. The effect of monovalent and divalent cations on the activity of *Streptococcus lactis* C10 pyruvate kinase. Biochim. Biophys. Acta **481:**105–114.
14. **De, B. K., J. S. Sampson, E. W. Ades, R. C. Huebner, D. L. Jue, S. E. Johnson, M. Espina, A. R. Stinson, D. E. Briles, and G. M. Carlone.** 2000. Purification and characterization of *Streptococcus pneumoniae* palmitoylated pneumococcal surface adhesin A expressed in *Escherichia coli*. Vaccine **18:**1811–1821.
15. **Dintilhac, A., G. Alloing, C. Granadel, and J. P. Claverys.** 1997. Competence and virulence of *Streptococcus pneumoniae*: Adc and PsaA mutants exhibit a requirement for Zn and Mn resulting from inactivation of putative ABC metal permeases. Mol. Microbiol. **25:**727–739.
16. **Drake, D., K. G. Taylor, and R. J. Doyle.** 1988. Expression of the glucan-binding lectin of *Streptococcus cricetus* requires manganous ion. Infect. Immun. **56:**2205–2207.
17. **Duane, P. G., J. B. Rubins, H. R. Weisel, and E. N. Janoff.** 1993. Identification of hydrogen peroxide as a *Streptococcus pneumoniae* toxin for rat alveolar epithelial cells. Infect. Immun. **61:**4392–4397.
18. **Flint, D. H., J. F. Tuminello, and M. H. Emptage.** 1993. The inactivation of Fe-S cluster containing hydro-lyases by superoxide. J. Biol. Chem. **268:**22369–22376.
19. **Froeliger, E. H., and P. Fives-Taylor.** 2000. *Streptococcus parasanguis* FimA does not contribute to adherence to SHA. J. Dent. Res. **79:**337.
20. **Giesbrecht, P., T. Kersten, H. Maidhof, and J. Wecke.** 1998. Staphylococcal cell wall: morphogenesis and fatal variations in the presence of penicillin. Microbiol. Mol. Biol. Rev. **62:**1371–1414.
21. **Gort, A. S., and J. A. Imlay.** 1998. Balance between endogenous superoxide stress and antioxidant defenses. J. Bacteriol. **180:**1402–1410.
22. **Havarstein, L. S., G. Coomaraswamy, and D. A. Morrison.** 1995. An unmodified heptadecapeptide pheromone induces competence for genetic transformation in *Streptococcus pneumoniae*. Proc. Natl. Acad. Sci. USA **92:**11140–11144.
23. **Higuchi, M.** 1992. Reduced nicotinamide adenine dinucleotide oxidase involvement in defense against oxygen toxicity of *Streptococcus mutans*. Oral Microbiol. Immunol. **7:**309–314.
24. **Holland, R., and G. G. Pritchard.** 1975. Regulation of the L-lactase dehydrogenase from *Lactobacillus casei* by fructose-1,6-diphosphate and metal ions. J. Bacteriol. **121:**777–784.
25. **Horsburgh, M. J., S. J. Wharton, M. Karavolos, and S. J. Foster.** 2002. Manganese: elemental defence for a life with oxygen. Trends Microbiol. **10:**496–501.
26. **Imlay, J. A.** 2003. Pathways of oxidative damage. Annu. Rev. Microbiol. **57:**395–418.
27. **Jakubovics, N. S., and H. F. Jenkinson.** 2001. Out of the iron age: new insights into the critical role of manganese homeostasis in bacteria. Microbiology **147:**1709–1718.
28. **Jakubovics, N. S., A. W. Smith, and H. F. Jenkinson.** 2000. Expression of the virulence-related Sca (Mn^{2+}) permease in *Streptococcus gordonii* is regulated by a diphtheria toxin metallorepressor-like protein ScaR. Mol. Microbiol. **38:**140–153.
29. **Jenkinson, H. F.** 1994. Cell surface protein receptors in oral streptococci. FEMS Microbiol. Lett. **121:**133–140.
30. **Keyer, K., and J. A. Imlay.** 1997. Inactivation of dehydratase [4Fe-4S] clusters and disruption of iron homeostasis upon cell exposure to peroxynitrite. J. Biol. Chem. **272:**27652–27659.
31. **Keyer, K., and J. A. Imlay.** 1996. Superoxide accelerates DNA damage by elevating free-iron levels. Proc. Natl. Acad. Sci. USA **93:**13635–13640.
32. **Kim, J. O., and J. N. Weiser.** 1998. Association of intrastrain phase variation in quantity of capsular polysaccharide and teichoic acid with the virulence of *Streptococcus pneumoniae*. J. Infect. Dis. **177:**368–377.
33. **Kolenbrander, P. E., and R. N. Andersen.** 1990. Characterization of *Streptococcus gordonii* (*S. sanguis*) PK488 adhesin-mediated coaggregation with *Actinomyces naeslundii* PK606. Infect. Immun. **58:**3064–3072.
34. **Kuo, C. F., T. Mashino, and I. Fridovich.** 1987. alpha, beta-Dihydroxyisovalerate dehydratase. A superoxide-sensitive enzyme. J. Biol. Chem. **262:**4724–4727.
35. **Lawrence, M. C., P. A. Pilling, V. C. Epa, A. M. Berry, A. D. Ogunniyi, and J. C. Paton.** 1998. The crystal structure of pneumococcal surface antigen PsaA reveals a metal-binding site and a novel structure for a putative ABC-type binding protein. Structure **6:**1553–1561.
36. **Letort, C., and V. Juillard.** 2001. Development of a minimal chemically-defined medium for the exponential growth of *Streptococcus thermophilus*. J. Appl. Microbiol. **91:**1023–1029.
37. **Lu, L., J. S. Singh, M. Y. Galperin, D. Drake, K. G. Taylor, and R. J. Doyle.** 1992. Chelating agents inhibit activity and prevent expression of streptococcal glucan-binding lectins. Infect. Immun. **60:**3807–3813.
38. **Marra, A., S. Lawson, J. S. Asundi, D. Brigham, and A. E. Hromockyj.** 2002. In vivo characterization of the *psa* genes from *Streptococcus pneumoniae* in multiple models of infection. Microbiology **148:**1483–1491.
39. **Mazmanian, S. K., H. Ton-That, and O. Schneewind.** 2001. Sortase-catalysed anchoring of surface proteins to the cell wall of Staphylococcus aureus. Mol. Microbiol. **40:**1049–1057.
40. **McDaniel, L. S., J. Yother, M. Vijayakumar, L. McGarry, W. R. Guild, and**

D. E. Briles. 1987. Use of insertional inactivation to facilitate studies of biological properties of pneumococcal surface protein A (PspA). J. Exp. Med. **165:**381–394.
41. **Morona, J. K., R. Morona, D. C. Miller, and J. C. Paton.** 2002. *Streptococcus pneumoniae* capsule biosynthesis protein CpsB is a novel manganese-dependent phosphotyrosine-protein phosphatase. J. Bacteriol. **184:**577–583.
42. **Niven, D. F., A. Ekins, and A. A. al-Samaurai.** 1999. Effects of iron and manganese availability on growth and production of superoxide dismutase by *Streptococcus suis*. Can. J. Microbiol. **45:**1027–1032.
43. **Novak, R., J. S. Braun, E. Charpentier, and E. Tuomanen.** 1998. Penicillin tolerance genes of *Streptococcus pneumoniae*: the ABC-type manganese permease complex Psa. Mol. Microbiol. **29:**1285–1296.
44. **Ogunniyi, A. D., R. L. Folland, D. E. Briles, S. K. Hollingshead, and J. C. Paton.** 2000. Immunization of mice with combinations of pneumococcal virulence proteins elicits enhanced protection against challenge with *Streptococcus pneumoniae*. Infect. Immun. **68:**3028–3033.
45. **Oligino, L., and P. Fives-Taylor.** 1993. Overexpression and purification of a fimbria-associated adhesin of *Streptococcus parasanguis*. Infect. Immun. **61:**1016–1022.
46. **Oliver, A. M., F. Martin, and J. F. Kearney.** 1999. IgMhighCD21high lymphocytes enriched in the splenic marginal zone generate effector cells more rapidly than the bulk of follicular B cells. J. Immunol. **162:**7198–7207.
47. **Pericone, C. D., K. Overweg, P. W. Hermans, and J. N. Weiser.** 2000. Inhibitory and bactericidal effects of hydrogen peroxide production by *Streptococcus pneumoniae* on other inhabitants of the upper respiratory tract. Infect. Immun. **68:**3990–3997.
48. **Pericone, C. D., S. Park, J. A. Imlay, and J. N. Weiser.** 2003. Factors contributing to hydrogen peroxide resistance in *Streptococcus pneumoniae* include pyruvate oxidase (SpxB) and avoidance of the toxic effects of the Fenton reaction. J. Bacteriol. **185:**6815–6825.
49. **Pierre, J. L., and M. Fontecave.** 1999. Iron and activated oxygen species in biology: the basic chemistry. Biometals **12:**195–199.
50. **Pilling, P. A., M. C. Lawrence, A. M. Berry, A. D. Ogunniyi, R. A. Lock, and J. C. Paton.** 1998. Expression, purification and preliminary X-ray crystallographic analysis of PsaA, a putative metal-transporter protein of *Streptococcus pneumoniae*. Acta Crystallogr. D Biol. Crystallogr. **54:**1464–1466.
51. **Posey, J. E., and F. C. Gherardini.** 2000. Lack of a role for iron in the Lyme disease pathogen. Science **288:**1651–1653.
52. **Ren, B., A. J. Szalai, O. Thomas, S. K. Hollingshead, and D. E. Briles.** 2003. Both family 1 and family 2 PspA proteins can inhibit complement deposition and confer virulence to a capsular serotype 3 strain of *Streptococcus pneumoniae*. Infect. Immun. **71:**75–85.
53. **Russell, H., J. A. Tharpe, D. E. Wells, E. H. White, and J. E. Johnson.** 1990. Monoclonal antibody recognizing a species-specific protein from *Streptococcus pneumoniae*. J. Clin. Microbiol. **28:**2191–2195.
54. **Scheuhammer, A. M., and M. G. Cherian.** 1985. Binding of manganese in human and rat plasma. Biochim. Biophys. Acta **840:**163–169.
55. **Schneewind, O., P. Model, and V. A. Fischetti.** 1992. Sorting of protein A to the staphylococcal cell wall. Cell **70:**267–281.
56. **Spellerberg, B., D. R. Cundell, J. Sandros, B. J. Pearce, I. Idanpaan-Heikkila, C. Rosenow, and H. R. Masure.** 1996. Pyruvate oxidase, as a determinant of virulence in *Streptococcus pneumoniae*. Mol. Microbiol. **19:**803–813.
57. **Tettelin, H., K. E. Nelson, I. T. Paulsen, J. A. Eisen, T. D. Read, S. Peterson, J. Heidelberg, R. T. DeBoy, D. H. Haft, R. J. Dodson, A. S. Durkin, M. Gwinn, J. F. Kolonay, W. C. Nelson, J. D. Peterson, L. A. Umayam, O. White, S. L. Salzberg, M. R. Lewis, D. Radune, E. Holtzapple, H. Khouri, A. M. Wolf, T. R. Utterback, C. L. Hansen, L. A. McDonald, T. V. Feldblyum, S. Angiuoli, T. Dickinson, E. K. Hickey, I. E. Holt, B. J. Loftus, F. Yang, H. O. Smith, J. C. Venter, B. A. Dougherty, D. A. Morrison, S. K. Hollingshead, and C. M. Fraser.** 2001. Complete genome sequence of a virulent isolate of Streptococcus pneumoniae. Science **293:**498–506.
58. **Tomasz, A.** 1981. Surface components of *Streptococcus pneumoniae*. Rev. Infect. Dis. **3:**190–211.
59. **Touati, D.** 2000. Iron and oxidative stress in bacteria. Arch. Biochem. Biophys. **373:**1–6.
60. **Tseng, H. J., A. G. McEwan, J. C. Paton, and M. P. Jennings.** 2002. Virulence of *Streptococcus pneumoniae*: PsaA mutants are hypersensitive to oxidative stress. Infect. Immun. **70:**1635–1639.
61. **Tseng, H. J., Y. Srikhanta, A. G. McEwan, and M. P. Jennings.** 2001. Accumulation of manganese in *Neisseria gonorrhoeae* correlates with resistance to oxidative killing by superoxide anion and is independent of superoxide dismutase activity. Mol. Microbiol. **40:**1175–1186.
62. **van de Rijn, I., and R. E. Kessler.** 1980. Growth characteristics of group A streptococci in a new chemically defined medium. Infect. Immun. **27:**444–448.
63. **Weinberg, E. D.** 1997. The Lactobacillus anomaly: total iron abstinence. Perspect. Biol. Med. **40:**578–583.
64. **Wu, H., K. P. Mintz, M. Ladha, and P. M. Fives-Taylor.** 1998. Isolation and characterization of Fap1, a fimbriae-associated adhesin of *Streptococcus parasanguis* FW213. Mol. Microbiol. **28:**487–500.
65. **Yesilkaya, H., A. Kadioglu, N. Gingles, J. E. Alexander, T. J. Mitchell, and P. W. Andrew.** 2000. Role of manganese-containing superoxide dismutase in oxidative stress and virulence of *Streptococcus pneumoniae*. Infect. Immun. **68:**2819–2826.
66. **Yother, J., G. L. Handsome, and D. E. Briles.** 1992. Truncated forms of PspA that are secreted from *Streptococcus pneumoniae* and their use in functional studies and cloning of the *pspA* gene. J. Bacteriol. **174:**610–618.
67. **Yother, J., L. S. McDaniel, and D. E. Briles.** 1986. Transformation of encapsulated *Streptococcus pneumoniae*. J. Bacteriol. **168:**1463–1465.
68. **Yother, J., and J. M. White.** 1994. Novel surface attachment mechanism of the *Streptococcus pneumoniae* protein PspA. J. Bacteriol. **176:**2976–2985.
69. **Yu, J., A. P. Bryant, A. Marra, M. A. Lonetto, K. A. Ingraham, A. F. Chalker, D. J. Holmes, D. Holden, M. Rosenberg, and D. McDevitt.** 2001. Characterization of the *Streptococcus pneumoniae* NADH oxidase that is required for infection. Microbiology **147:**431–438.

Editor: J. N. Weiser